

Rashba spin-orbit coupling induced rectified currents in monolayer graphene with exchange field and sublattice potential

Liang Chen(陈亮), Feng Li(李峰), and Xiao-Ming Ding(丁晓明)

Citation: Chin. Phys. B, 2023, 32 (**8**): 087103. DOI: 10.1088/1674-1056/acc932
Journal homepage: http://cpb.iphy.ac.cn; http://iopscience.iop.org/cpb

What follows is a list of articles you may be interested in

A sport and a pastime: Model design and computation in quantum many-body systems

Gaopei Pan(潘高培), Weilun Jiang(姜伟伦), and Zi Yang Meng(孟子杨)
Chin. Phys. B, 2022, 31 (**12**): 127101. DOI: 10.1088/1674-1056/aca083

Robust and intrinsic type-III nodal points in a diamond-like lattice

Qing-Ya Cheng(程青亚), Yue-E Xie(谢月娥), Xiao-Hong Yan(颜晓红), and Yuan-Ping Chen(陈元平)
Chin. Phys. B, 2022, 31 (**11**): 117101. DOI: 10.1088/1674-1056/ac7c00

Modulation of Schottky barrier in XSi$_2$N$_4$/graphene (X=Mo and W) heterojunctions by biaxial strain

Qian Liang(梁前), Xiang-Yan Luo(罗祥燕), Yi-Xin Wang(王熠欣), Yong-Chao Liang(梁永超), and Quan Xie(谢泉)
Chin. Phys. B, 2022, 31 (**8**): 087101. DOI: 10.1088/1674-1056/ac5c3b

TiS_2-graphene heterostructures enabling polysulfide anchoring and fast electrocatalyst for lithium-sulfur batteries: A first-principles calculation

Wenyang Zhao(赵文阳), Li-Chun Xu(徐利春), Yuhong Guo(郭宇宏), Zhi Yang(杨致), Ruiping Liu(刘瑞萍), and Xiuyan Li(李秀燕)
Chin. Phys. B, 2022, 31 (**4**): 047101. DOI: 10.1088/1674-1056/ac3227

Magnetic and electronic properties of two-dimensional metal-organic frameworks $TM_3(C_2NH)_{12}$

Zhen Feng(冯振), Yi Li(李依), Yaqiang Ma(马亚强), Yipeng An(安义鹏), and Xianqi Dai(戴宪起)
Chin. Phys. B, 2021, 30 (**9**): 097102. DOI: 10.1088/1674-1056/ac0cdb

---

Rashba spin–orbit coupling induced rectified currents in monolayer graphene with exchange field and sublattice potential

Liang Chen(陈亮)[†], Feng Li(李峰), and Xiao-Ming Ding(丁晓明)

School of Physics and Electronic Engineering, Taishan University, Taian 271000, *China*

(Received 22 September 2022; revised manuscript received 30 March 2023; accepted manuscript online 31 March 2023)

We investigate the effect of Rashba spin–orbit coupling (RSOC) on photoconductivities of rectified currents in monolayer graphene with exchange field and sublattice potential. The system shows that the photoconductivities of resonant shift and injection current contributions are nonzero, while the photoconductivities of non-resonant shift current contribution are zero. We find that the RSOC induces a warping term, which leads to the nonzero rectified currents. Moreover, the photoconductivities of resonant injection (shift) current contribution are (not) related to the relaxation rate. The similar behavior can be found in other Dirac materials, and our findings provide a way to tune the nonlinear transport properties of Dirac materials.

Keywords: graphene, spin orbit coupling, shift current, inject current

PACS: 71.70.Ej, 81.05.Ue **DOI:** 10.1088/1674-1056/acc932

1. Introduction

Graphene has attracted a great deal of attention in recent years because it emerged as the first truly two-dimensional crystal ever discovered.[1] Its unique band structure, high electronic mobility, and ultra-thin dimensionality make it become a unique material for exploring transport properties,[2,3] which is important to the future generation of nanoelectronic and nanophotonic devices. Understanding the transport properties of graphene is critical to realize the corresponding applications. Various physical mechanisms about engineering transport in graphene have been studied, including disorder, interaction, magnetic field, spin–orbit coupling (SOC), strain, and so on. Quantum anomalous Hall conductivity,[4,5] spin Hall conductivity,[6,7] and valley Hall conductivity[8–10] in graphene are intimately related to the topological properties of the system. Recently, Hall effect in strained graphene has become a new active field of research.[11] Moreover, some recent works have investigated nonlinear transport in graphene.[12–18] Nonlinear optical conductivity in graphene has been studied by solving the Bloch equation.[15,16] Mikhailov[17] has developed an analytical theory of the third-order nonlinear effects and calculated the local third-order conductivity in graphene. However, the rectified current resulted from spatially uniform ac electric field in graphene has rarely been taken into account.

On the other hand, two-dimensional materials with SOC have attracted wide interests due to the possibility of controlling and manipulating both electronic and spin transports in various optoelectronic and spintronic devices. The intrinsic SOC of graphene is present when an inversion symmetry with respect to graphene plane is broken. The Rashba spin–orbit coupling (RSOC) arises when the electric field is applied perpendicular to the graphene layer. In graphene, the intrinsic SOC and RSOC are weak. However, recent works have suggested that the RSOC can be strong. A much stronger RSOC can be induced in a graphene layer which is deposited on a heavy metal substrate.[19,20] Balakrishnan *et al.*[21] have demonstrated that the RSOC interaction in graphene can be markedly enhanced by introducing a small concentration of covalently bonded adatoms. First-principles calculations have also predicted that strong RSOC can be induced by hydrogen adatom on graphene.[22] By proximity coupling with exfoliated transition metal dichalcogenides or WS_2, strong RSOC can be acquired in graphene.[23,24]

In this article, we study the effect of RSOC on nonlinear transport properties of monolayer graphene with exchange field and sublattice potential. We focus upon the effect of RSOC on rectified currents in monolayer graphene with exchange field and sublattice potential. The RSOC can induce a warping term in gapped monolayer graphene, which leads to the nonzero photoconductivities of resonant shift and injection current contributions.

This paper is organized as follows. In Section 2, we firstly describe the model with RSOC, analyze the band structure, and present the low-energy effective model. In Sections 2 and 3, we provide the results of photoconductivities of resonant shift and injection current contributions with RSOC. Finally, we give a brief conclusion in Section 5.

2. Model and formula

2.1. Model Hamiltonian

In the tight-binding approximation, the Hamiltonian for graphene in the presence of RSOC, exchange field, and sub-

[†]Corresponding author. E-mail: tsuchenliang@tsu.edu.cn

© 2023 Chinese Physical Society and IOP Publishing Ltd

lattice potential is written as[25]

$$H = -t\sum_{\langle ij\rangle\alpha} c^{\dagger}_{i\alpha}c_{j\alpha} + \mathrm{i}\lambda_{\mathrm{R}}\sum_{\langle ij\rangle\alpha\beta} c^{\dagger}_{i\alpha}(\boldsymbol{s}\times\boldsymbol{d}_{ij})^{z}_{\alpha\beta}c_{j\beta} + M\sum_{i\alpha\beta} c^{\dagger}_{i\alpha}s^{z}_{\alpha\beta}c_{i\alpha\beta} + \Delta\sum_{i\alpha}\mu_i c^{\dagger}_{i\alpha}c_{i\alpha}. \quad (1)$$

Here, $c^{\dagger}_{i\alpha}$ and $c_{i\alpha}$ are creation and annihilation operators for an electron with spin α on site i. The first term is the usual nearest-neighbor hopping term, and $\langle\ \rangle$ runs over all the nearest-neighbor hopping sites. The second term represents extrinsic RSOC terms, and $\boldsymbol{d}_{ij}$ is the unit vector pointing from site j to i. The third term denotes the exchange field. The last term corresponds to the staggered sublattice potential, and $\mu_i = \pm 1$ depends on the A/B sublattice. Figures 1(a) and 1(b) show the distribution of energy in momentum space near the corners of the Brillouin zone without and with RSOC at $M = \Delta = 0$, respectively. When RSOC is present, the energy bands have a threefold rotational symmetry near the corners of the Brillouin zone. The RSOC induces a warping term in monolayer graphene, which deforms Fermi surface. Due to the change of energy band dispersion and corresponding eigenvector, the group velocity is modified. Therefore, the RSOC induces important modifications on Berry curvature, and the corresponding transport properties will be changed.

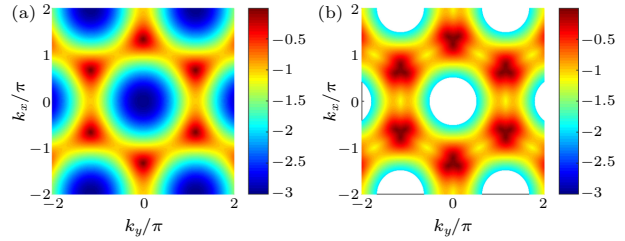


Fig. 1. Distribution of energy in momentum space near the corners of the Brillouin zone without (a) and with (b) Rashba spin–orbit coupling at $M = \Delta = 0$.

In order to further analyze the physics of the electronic behavior near the Dirac cones, we start our discussion about the effective low-energy Hamiltonian. In the presence of extrinsic RSOC and $|M| \simeq |\Delta|$, the low-energy effective Hamiltonian of our system can be written as[26,27]

$$H(\boldsymbol{k}) = \boldsymbol{d}(\boldsymbol{k})\cdot\hat{\boldsymbol{\sigma}}, \quad (2)$$

where $\boldsymbol{d} = (d_x(\boldsymbol{k}), d_y(\boldsymbol{k}), d_z(\boldsymbol{k}))$, $\hat{\boldsymbol{\sigma}} = (\sigma_x, \sigma_y, \sigma_z)$, $d_x(\boldsymbol{k}) = -v_{\mathrm{so}}(k_y + 2\sqrt{3}\eta\Lambda k_x k_y)$, $d_y(\boldsymbol{k}) = v_{\mathrm{so}}[\eta k_x + \sqrt{3}\Lambda(k_y^2 - k_x^2)]$, $d_z(\boldsymbol{k}) = \Delta - \eta M(1 - \Lambda k^2)$; $v_{\mathrm{so}} = \sqrt{3}\lambda_{\mathrm{R}}/2$, $\eta = \mathrm{sgn}(\Delta M)$, and $\Lambda = 2v_{\mathrm{F}}^2/(4|M\Delta| + 9\lambda_{\mathrm{R}}^2)$. The corresponding eigenvalues and eigenvectors are given as follows:

$$E_n^{\eta} = (-1)^n\sqrt{d_x^2 + d_y^2 + d_z^2} = (-1)^n\sqrt{v_{\mathrm{so}}^2k^2 + 3v_{\mathrm{so}}^2\Lambda^2k^4 + 2\sqrt{3}\eta v_{\mathrm{so}}^2\Lambda k_x(3k_y^2 - k_x^2) + d_z^2}, \quad (3)$$

$$|1\rangle = \left[\sin\frac{\alpha}{2}\mathrm{e}^{-\mathrm{i}\phi},\ -\cos\frac{\alpha}{2}\right]^{\mathrm{T}}, \quad (4)$$

$$|2\rangle = \left[\cos\frac{\alpha}{2},\ \sin\frac{\alpha}{2}\mathrm{e}^{\mathrm{i}\phi}\right]^{\mathrm{T}}, \quad (5)$$

where $n = 1, 2$ denote the valence and conduction bands, superscript T denotes the transpose of the matrix, $\tan\alpha = \sqrt{d_x^2 + d_y^2}/d_z$, and $\tan\phi = d_y/d_x$. In Eq. (3), $\cos\theta(3\sin^2\theta - \cos\theta^2) = -\cos(3\theta)$, the bands are threefold rotational symmetry, which is in agreement with Fig. 1(b). Therefore, the low-energy effective Hamiltonian (2) is enough to capture the physics in our system.

2.2. Rectified current formula

Based on nonequilibrium Green's function technique and Floquet's theory,[28,29] the rectified currents responding to oscillating electric fields in monolayer graphene at $|M| \simeq |\Delta|$ can be decomposed into three contributions, i.e.,

$$J = J_1 + J_2 + J_3, \quad (6)$$

$$J_1 = \frac{e}{\hbar}\int\frac{\mathrm{d}^2k}{(2\pi)^2}\frac{\frac{\Gamma}{2}(f_{\mathrm{v}} - f_{\mathrm{c}})}{h^2 + \Gamma^2/4}(h_y v_x - v_y h_x), \quad (7)$$

$$J_2 = \frac{e}{\hbar}\int\frac{\mathrm{d}^2k}{(2\pi)^2}\frac{h_z(f_{\mathrm{v}} - f_{\mathrm{c}})}{h^2 + \Gamma^2/4}(h_x v_x + v_y h_y), \quad (8)$$

$$J_3 = \frac{e}{\hbar}\int\frac{\mathrm{d}^2k}{(2\pi)^2}\frac{h_x^2 + h_y^2}{h^2 + \Gamma^2/4}v_z(f_{\mathrm{v}} - f_{\mathrm{c}}). \quad (9)$$

Here, the three terms denote the resonant shift current, the non-resonant shift current, and the resonant injection current; f is the Fermi–Dirac distribution function, subscripts v and c stand for valence and conduction bands, respectively; and Γ is the relaxation rate. We consider that the electric field and Γ are small. Therefore, $h_x - \mathrm{i}h_y = \mathrm{i}\frac{eE}{\hbar\omega}(\frac{\partial H}{\partial k})_{\mathrm{v,c}}$, $h_z = (E_1^{\eta} - E_2^{\eta} + \hbar\omega)/2$, $v_x - \mathrm{i}v_y = \mathrm{i}\frac{eE}{\hbar\omega}(\frac{\partial^2 H}{\partial_k\partial k})_{\mathrm{v,c}}$, and $v_z = \partial_k(E_1^{\eta} - E_2^{\eta})/2$. In next sections, we will discuss the effect of RSOC on the three contributions.

3. Shift current

In this section, we investigate the resonant and non-resonant shift currents in monolayer graphene with RSOC when $|M| \simeq |\Delta|$. In the perturbative regime, the photoconductivities of resonant shift current (J_1) and non-resonant shift current (J_2) can be rewritten as[28]

$$\sigma^{ii}_{\mathrm{rsc}}(\omega) = \frac{e^3}{\hbar\omega^2}\int\frac{\mathrm{d}^2k}{(2\pi)^2}\frac{\Gamma/2}{(E_{\mathrm{c}}^{\eta} - E_{\mathrm{v}}^{\eta} - \hbar\omega)^2 + \frac{\Gamma^2}{4}}|v^i_{\mathrm{v,c}}|^2R^i, \quad (10)$$

$$\sigma^{ij}_{\mathrm{nrsc}}(\omega) = \frac{e^3}{\hbar\omega^2}\int\frac{\mathrm{d}^2k}{(2\pi)^2}\mathrm{Re}\left\{v^i_{\mathrm{v,c}}\left(\frac{\partial v^i}{\partial k_j}\right)_{\mathrm{c,v}}\right\} \times\frac{E_{\mathrm{c}}^{\eta} - E_{\mathrm{v}}^{\eta} - \hbar\omega}{(E_{\mathrm{c}}^{\eta} - E_{\mathrm{v}}^{\eta} - \hbar\omega)^2 + \frac{\Gamma^2}{4}}. \quad (11)$$

Here, $v^i_{\mathrm{v,c}}$ represents the matrix elements of velocity along i direction corresponding to conduct and valence bands; $R^i =$

$\partial_i\phi^i_{\rm c,v}+r^a_{\rm c,c}-r^a_{\rm v,v}$ is the shift vector; $\phi^i_{\rm c,v}$ is the phase factor of the Berry connection $r^i_{\rm c,v}$; and $r^i_{nm}=\mathrm{i}\langle n|\partial_i m\rangle$ is the Berry connection between energy bands n and m.

Furthermore, the electric field is assumed to be sufficiently small, $\frac{\Gamma/2}{(E^\eta_{\rm c}-E^\eta_{\rm v}-\hbar\omega)^2+\frac{\Gamma^2}{4}}\approx\pi\delta(E^\eta_{\rm c}-E^\eta_{\rm v}-\hbar\omega)$ is obtained. Then we get

$$\sigma^{ii}_{\rm rsc}(\omega)=\frac{\pi e^3}{\hbar\omega^2}\int\frac{\mathrm{d}^2k}{(2\pi)^2}|v^i_{\rm v,c}|^2R^i\delta(E^\eta_{\rm c}-E^\eta_{\rm v}-\hbar\omega),\quad(12)$$

which is in accord with the results in Refs. [30–32], and

$$\sigma^{ij}_{\rm nrsc}(\omega)=0.\quad(13)$$

Figure 2(a) shows the photoconductivities of shift current $\sigma^{yy}_{\rm rsc}(\omega)$ as a function of ω in units of $\sigma_0=2e^3/\hbar$ for $\lambda_{\rm R}=0.2t$ and $\Delta=0.2t$ at $M=0.18t$ (red curve) and $M=-0.18t$ (blue-dashed curve). When the RSOC is absent, the photoconductivity of shift current is zero, which can be confirmed by straightforwardly calculating $R^i=0$ of $H_{\lambda_{\rm R}=0}=v_{\rm F}(\tau k_x\sigma_x+k_y\sigma_y)+\Delta\sigma_z+sM$. In the presence of RSOC, the RSOC induces a warping term [see Eq. (2)], which modifies the velocity $v^i_{\rm v,c}$ between conduct and valence bands. Moreover, $R^i=-\frac{1}{4}[(\partial_a\alpha)^2+\sin^2\alpha(\partial_a\phi)^2]\neq0$. Therefore, Fig. 2(a) shows that nonzero $\sigma^{yy}_{\rm rsc}(\omega)$ emerges suddenly at the top of the valence band, and decreases with the ω. Finally, $\sigma^{yy}_{\rm rsc}(\omega)$ disappears at larger ω. Moreover, the amplitude of $\sigma^{yy}_{\rm rsc}(\omega)$ can be controlled by changing the sign of M. For fixed ω, $\sigma^{yy}_{\rm rsc}(\omega)$ increases with the strength of RSOC [see Fig. 2(b)].

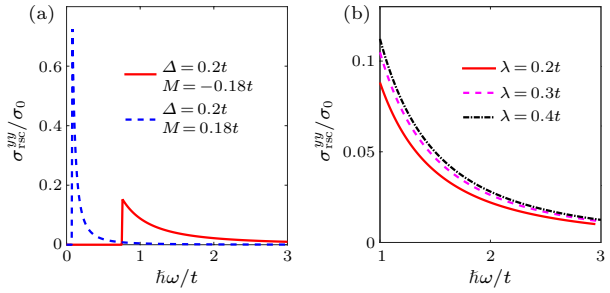


Fig. 2. (a) Photoconductivities of shift current $\sigma^{yy}_{\rm rsc}$ dependent on ω in units of $\sigma_0=2e^3/\hbar$ at $\lambda_{\rm R}=0.2t$, $\Delta=0.2t$, $M=0.18t$ (blue-dashed curve), and $M=-0.18t$ (red curve) respectively; (b) $\sigma^{yy}_{\rm rsc}$ dependent on ω at $M=-0.18t$ and $\Delta=0.2t$ with $\lambda_{\rm R}=0.2t$ (red curve), $\lambda_{\rm R}=0.3t$ (dashed magenta curve), and $\lambda_{\rm R}=0.4t$ (dash-dotted black curve).

4. Resonant injection current

In this section, we investigate the resonant inject current in monolayer graphene with RSOC when $|M|\simeq|\Delta|$. In the perturbative regime, the photoconductivity of resonant injection current (J_3) for sufficiently small electric field can be rewritten as

$$\sigma^{ii}_{\rm ric}(\omega)=\frac{\pi e^3}{2\hbar\omega^2}\int\frac{\mathrm{d}^2k}{(2\pi)^2}\frac{\partial_iE^\eta_{\rm c}-\partial_iE^\eta_{\rm v}}{(E^\eta_{\rm c}-E^\eta_{\rm v}-\hbar\omega)^2+\frac{\Gamma^2}{4}}|v^i_{\rm v,c}|^2$$
$$\approx\frac{e^3}{\Gamma\hbar\omega^2}\int\frac{\mathrm{d}^2k}{(2\pi)^2}|v^i_{\rm v,c}|^2(\partial_iE^\eta_{\rm c}-\partial_iE^\eta_{\rm v})$$
$$\times\delta(E^\eta_{\rm c}-E^\eta_{\rm v}-\hbar\omega).\quad(14)$$

When the RSOC is absent, the photoconductivities of resonant injection current, $\sigma^{yy}_{\rm ric}(\omega)$, is zero due to $|v^i_{\rm v,c}|^2(\partial_iE^\eta_{\rm c}-\partial_iE^\eta_{\rm v})\sim k^2k_i^3$. Figure 3(a) shows the photoconductivities of resonant injection current, $\sigma^{yy}_{\rm rsc}(\omega)$, as a function of ω in units of $\sigma_{0ic}=2e^3/\hbar\Gamma$ for $\lambda_{\rm R}=0.2t$ and $\Delta=0.2t$ at $M=0.18t$ (red curve) and $M=-0.18t$ (blue-dashed curve), when the RSOC is included. When ω sweeps the top of the valence band, $\sigma^{yy}_{\rm ric}(\omega)$ exhibits a peak, and then decreases with the ω. At larger ω, the effect of RSOC is negligible due to the large momentum. Therefore, $\sigma^{yy}_{\rm ric}(\omega)$ disappears. Moreover, the amplitude of $\sigma^{yy}_{\rm ric}(\omega)$ can be changed with reversing the sign of M. These behaviors are similar to $\sigma^{yy}_{\rm rsc}(\omega)$. However, $\sigma^{yy}_{\rm ric}(\omega)$ is related to Γ, while $\sigma^{yy}_{\rm rsc}(\omega)$ is not. For fixed ω, Fig. 3(b) shows that $\sigma^{yy}_{\rm ric}(\omega)$ increases with the strength of RSOC.

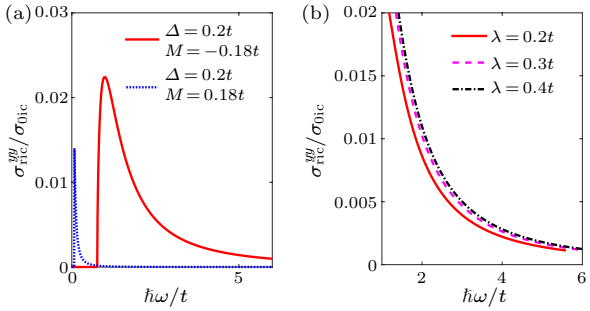


Fig. 3. (a) Photoconductivities of inject current, $\sigma^{yy}_{\rm nic}$, dependent on ω in units of $\sigma_{0ic}=2e^3/\hbar\Gamma$ at $\lambda_{\rm R}=0.2t$, $\Delta=0.2t$, $M=0.18t$ (blue-dashed curve), and $M=-0.18t$ (red curve); (b) $\sigma^{yy}_{\rm nic}$ dependent on ω at $M=-0.18t$ and $\Delta=0.2t$ with $\lambda_{\rm R}=0.2t$ (red curve), $\lambda_{\rm R}=0.3t$ (dashed magenta curve), and $\lambda_{\rm R}=0.4t$ (dash-dotted black curve).

5. Conclusions

In summary, we have studied the photoconductivities of rectified currents in monolayer graphene with exchange field and sublattice potential due to the Rashba spin–orbit coupling (RSOC). Our results show that there are nonzero photoconductivities of resonant shift and injection current contributions, and zero photoconductivities of non-resonant shift current contribution. Moreover, the photoconductivities of injection current contribution are related to the relaxation rate, while the photoconductivities of resonant shift current contribution are not. The photoconductivities of resonant injection and shift current contributions can be controlled by the interplay between exchange field and sublattice potential. The RSOC in our system leads to a warping term [see Eq. (2)], which has an essential role for the rectified current. The warping term can also be found in other Dirac materials including strained graphene[33] and monolayer MoS_2.[34,35] The similar nonlinear behavior can be found in other Dirac materials, and our findings are useful in explaining the effect of RSOC on engineering the nonlinear transport properties in monolayer graphene and other Dirac materials.

Acknowledgement

Project supported by the Shandong Province Natural Science Foundation (Grant No. ZR2021MF077).

References

[1] Novoselov K S, Geim A K, Morozov S V, Jiang D, Zhang Y, Dubonos S V, Grigorieva I V and Firsov A A 2004 *Science* **306** 666
[2] Peres N M R 2010 *Phys. Mod. Rev.* **82** 2673
[3] Sarma S D, Adam S, Hwang E H and Rossi E 2011 *Phys. Mod. Rev.* **83** 407
[4] Qiao Z, Yang S A, Feng W, Tse W K, Ding J, Yao Y, Wang J and Niu Q 2010 *Phys. Rev. B* **82** 161414
[5] Li Z and Wang Z F 2020 *Chin. Phys. B* **29** 107101
[6] Kane C L and Mele E J 2005 *Phys. Rev. Lett.* **95** 226801
[7] Sinitsyn N A, Hill J E, Min H, Sinova J and MacDonald A H 2006 *Phys. Rev. Lett.* **97** 106804
[8] Lee K W and Lee C E 2017 *Phys. Rev. B* **95** 085145
[9] Martiny J H J, Kaasbjerg K and Jauho A P 2019 *Phys. Rev. B* **100** 155414
[10] Lü X Y and Li Z Qiang 2019 *Acta Phys. Sin.* **68** 220303 (in Chinese)
[11] Naumis G G, Barraza-Lopez S, Oliva-Leyva M and Terrones Hu 2017 *Rep. Prog. Phys.* **80** 096501
[12] Mikhailov S A and Ziegler K 2007 *J. Phys.: Condens. Matter* **20** 384204
[13] Hendry E, Hale P J, Moger J, Savchenko A K and Mikhailov S A 2010 *Phys. Rev. Lett.* **105** 097401
[14] Kumar N, Kumar J, Gerstenkorn C, Wang R, Chiu H Y, Smirl A L and Zhao H 2013 *Phys. Rev. B* **87** 121406
[15] Cheng J L, Vermeulen N and Sipe J E 2015 *Phys. Rev. B* **91** 235320
[16] Singh A, Bolotin K I, Ghosh S and Agarwal A 2017 *Phys. Rev. B* **95** 155421
[17] Mikhailov S A 2016 *Phys. Rev. B* **93** 085403
[18] Guan Z, Liu L, Wang G L, Zhao S F, Jiao Z H and Zhou X X 2020 *Chin. Phys. B* **29** 104206
[19] Varykhalov A, Sánchez-Barriga J, Shikin A M, Biswas C, Vescovo E, Rybkin A, Marchenko D and Rader O 2008 *Phys. Rev. Lett.* **101** 157601
[20] Marchenko D, Varykhalov A, Scholz M R, Bihlmayer G, Rashba EI, Rybkin A, Shikin A M and Rader O 2012 *Nat. Commun.* **3** 1232
[21] Balakrishnan J, Koon G K W, Jaiswal M, Castro Neto A H and Özyilmaz B 2013 *Nat. Phys.* **9** 284
[22] Gmitra M, Kochan D and Fabian J 2013 *Phys. Rev. Lett.* **110** 246602
[23] Wang Z, Ki D K, Chen H, Berger H, MacDonald A H and Morpurgo A F 2015 *Nat. Commun.* **6** 8339
[24] Yang B, Lohmann M, Barroso D, Liao I, Lin Z, Liu Y, Bartels L, Watanabe K, Taniguchi T and Shi J 2017 *Phys. Rev. B* **96** 041409
[25] Qiao Z, Jiang H, Li X, Yao Y and Niu Q 2012 *Phys. Rev. B* **85** 115439
[26] Yu Z, Pan H and Yao Y 2015 *Phys. Rev. B* **92** 155419
[27] Liu C C, Jiang H and Yao Y 2011 *Phys. Rev. B* **84** 195430
[28] Morimoto1 T and Nagaosa N 2016 *Sci. Adv.* **2** 1501524
[29] Matsyshyn O, Piazza F, Moessner R and Sodemann I 2021 *Phys. Rev. Lett.* **127** 126604
[30] Cook A M, Fregoso B M, Juan F d, Coh S and Moore J E 2017 *Nat. Commun.* **8** 14176
[31] Sipe J E and Shkrebtii A I 2000 *Phys. Rev. B* **61** 5337
[32] Mahmoudi F and Asgari R 2022 *Phys. Rev. B* **105** 085403
[33] Battilomo R, Scopigno N and Ortix C 2019 *Phys. Rev. Lett.* **123** 196403
[34] Kormányos A, Zólyomi V, Drummond N D, Rakyta P, Burkard G and Fal' ko V I 2008 *Phys. Rev. B* **88** 045416
[35] Liu G B, Shan W Y, Yao Y, Yao W and Xiao D 2008 *Phys. Rev. B* **88** 085433